Molecular Dynamics Simulation of Surfactin Molecules at the Water-Hexane Interface

J. P. Nicolas
Department of Chemical Engineering, University of Amsterdam, Amsterdam, The Netherlands

ABSTRACT The dynamics of surfactin, a lipopeptide surfactant from *Bacillus subtilis*, has been studied by molecular dynamics at different interfacial concentrations in a water-hexane medium reproducing a hydrophilic/hydrophobic biphasic system. The shapes and orientations of surfactin molecules, as hydrogen bonds and Ramachandran angles, have been recorded to investigate the environment effect on the molecular structure. We demonstrate that the peptidic backbone can exhibit a large flexibility and that conformational motions and structural fluctuations depend strongly on the interfacial concentration. Moreover, we have measured the surface activity of this biosurfactant by computing the interfacial tension and lateral and rotational diffusion coefficients.

INTRODUCTION

Surfactin is an amphiphilic lipopeptide produced by various strains of *Bacillus subtilis* (Arima et al., 1968) and consists of a heptaptide headgroup with the sequence Glu-Leu-*D*Leu-Val-Asp-*D*Leu-Leu linked to a $RC_{14–15}$ β-hydroxy fatty acid (Nagai et al., 1996) and closed by a lactone ring. Surfactin is a powerful biodegradable surfactant lowering water surface tension from 72 to ~30 mN/m at concentrations of ~10 μM (Ishigami et al., 1995; Peypoux et al., 1999). At very low concentrations it forms large micelles and the critical micellar concentration of the different analogs is of the order 10^{-5} M (Ishigami et al., 1995). Besides its interfacial properties, surfactin exhibits several biological activities: antibacterial (Vollenbroich et al., 1997b; Béven and Wróblewski, 1997), hemolytic (Kracht et al., 1999), antiviral (Kracht et al., 1999; Vollenbroich et al., 1997a), and antitumoral (Kameda et al., 1974). Surfactin interacts with membranes (Maget-Dana and Ptak, 1992), initiates lipid phase transitions (Grau et al., 1999), and membrane destabilization (Heerklotz and Seelig, 2001). Such surface and biological properties have attracted interest in the structure of surfactin and its behavior at hydrophilic/hydrophobic interfaces.

From ^{1}H-NMR studies correlated to distance geometry, energy minimization, and molecular dynamics techniques, a first three-dimensional structure for surfactin in DMSO has been proposed (Bonmatin et al., 1994). Two models were presented where in both cases the peptidic moiety adopts a ''horse-saddle'' conformation with the two hydrophilic residues pointing on one side forming a potentially binding ''claw'' and the five hydrophobic ones associated to the fatty acid chain pointing on the other side. The two structures differ mainly from their intramolecular hydrogen bonds, [NH(5)-CO(2)] and [NH(7)-CO(5), NH(4)-CO(2), and NH(6)-C_1O] for S1 and S2 structures, respectively. Structure-activity correlation has been extensively studied during micelle formation (Ishigami et al., 1995; Osman et al., 1998), by Fourier transform infrared spectroscopy and circular dichroism in various solvent systems (Ferré et al., 1997; Vass et al., 2001), and at air/water interface (Razafindralambo et al., 1997, 1998) and hydrophobic/hydrophilic mimicking medium (Gallet et al., 1999). All those recent results suggest a flexibility of the backbone conformational structure and several stable configurations are proposed and debated.

The purpose of our work was to explore the conformation flexibility of surfactin for various interfacial concentrations in a hydrophilic/hydrophobic medium similar to a biological system as lipid/water interface. To avoid perturbations resulting from such aliphatic chain order and lipid headgroup interactions, we have mimicked this environment with an amorphous hexane/water system described at an atomic scale. Furthermore, we have computed the effect of adding biosurfactant on the interfacial tension at the oil/water interface and estimated the lateral and rotational diffusion coefficients.

METHODOLOGY

Molecular dynamics

Simulations

Molecular dynamics computer simulations were carried out using the DLPOLY package (2001). An all atom model was employed to describe molecules at an atomic scale using the potential energy parameter set PARM27 from the CHARMM package (MacKerell et al., 1998). The TIP3P water model (Jorgensen et al., 1983) was used in all simulations. Bonds involving hydrogen were held fixed with the SHAKE algorithm (Ryckaert et al., 1977). Electrostatic interactions were computed using the Smooth Particle Mesh Ewald method (Essmann et al., 1995). Our simulations were

Submitted December 18, 2002, and accepted for publication April 10, 2003.

Address reprint requests to J. P. Nicolas, Dept. of Chemical Engineering, University of Amsterdam, Nieuwe Achtergracht 166, 1018WV Amsterdam, The Netherlands. Tel.: 31-20-525-6492; Fax: 31-20-525-5604; E-mail: jpierre@science.uva.nl.

0006-3495/03/09/1377/15 $2.00

performed in the NVT ensemble (Hoover, 1985), i.e., with constant temperature, volume, and number of particles. The equations of motions were solved using the Verlet Leapfrog integration algorithm (Allen and Tildesley, 1989) and simulations were run with periodic boundary conditions. All the simulations were performed using a cutoff radius of 12 Å for the van der Waals terms.

Initially, a single protonated surfactin molecule was equilibrated in vacuum. Bonmatin has kindly provided the coordinates of the S1 and S2 heptapeptide conformers of the surfactin molecule which have been completed with a *R*-C_{14} β-hydroxy fatty acid chain (Nagai et al., 1996). The analysis of those conformers with hydrogen bond criteria (Thornton et al., 1993; MacDonald and Thornton, 1994) shows that S1 exhibit a β-turn type II′ *Asp*5 → *Leu*2 with two hydrogen bonds CO(5)-NH(2) and NH(5)-CO(2), while S2 contains two reverse γ-turns centered on the *D*-residues with their respective hydrogen bond, *Val*4 → *Leu*2 and *Leu*7 → *Asp*5, and a third hydrogen bond NH(6)-C_1O. After this preliminary protonated structure relaxation, we have built our complete models in three steps. First, we have equilibrated a box containing two phases, liquid hexane and vacuum, with interfaces parallel to the *x*-*y* plane. Subsequently, surfactin molecules have been added into the box, with the fatty-acid chain inserted in liquid hexane phase and the heptapeptide moiety at the interface. A few runs of equilibration were carried out with a very small timestep, which was gradually increased until a final value of 2 fs. Finally, the boxes were filled by adding water molecules. In such a way systems were prepared containing 448 hexane molecules, 2, 4, 8, 18, 24, or 32 molecules of surfactin (corresponding to 1, 2, 4, 9, 12, or 16 molecules per interface, respectively), and ~2000 molecules of water, thus ~17,000 atoms. The box dimensions were $45 \times 45 \times L_z$ Å in the *x*-, *y*-, and *z*-directions, respectively, with $L_z \approx 93$ Å. These systems have been equilibrated for 100.000 steps, with a timestep of 2 fs at a temperature of 303 K. During equilibration, density profiles and energy convergence of the system have been monitored. After equilibration, we have recorded the dynamics of the system by accumulating coordinates at an interval of 0.4 ps during two periods of 0.5 ns.

Interfacial tension calculation

The interfacial tension γ is proportional to the integral of the difference between the normal $P_N(z)$ and tangential $P_T(z)$ components of the pressure tensor. For an interface normal to the *z*-axis, the expression for the interfacial tension reads:

$$\gamma = \frac{1}{2}\int_{-L_z/2}^{+L_z/2} dz[P_N(z) - P_T(z)], \qquad (1)$$

where L_z is the length of the simulation box along the *z*-axis, perpendicular to liquid-liquid interfaces, and the factor $1/2$ is a correction factor to take into account that the simulation boxes contain two interfaces.

The components of the pressure tensor are computed as a function of the distance to the interface using the Irving and Kirkwood definition (Walton et al., 1983; Kirkwood and Buff, 1949):

$$P_T(z) = \langle\rho(z)\rangle k_B T - \frac{1}{A}\left\langle \sum_i \sum_{j>i} \frac{(x_{ij}^2 + y_{ij}^2)}{2r_{ij}} \frac{dU_{int.}(r_{ij})}{dr_{ij}} \frac{1}{|z_{ij}|} \times \theta\left(\frac{z - z_i}{z_{ij}}\right)\theta\left(\frac{z_{ij}}{z_j - z}\right)\right\rangle, \qquad (2)$$

$$P_N(z) = \langle\rho(z)\rangle k_B T - \frac{1}{A}\left\langle \sum_i \sum_{j>i} \frac{z_{ij}^2}{2r_{ij}} \frac{dU_{int.}(r_{ij})}{dr_{ij}} \frac{1}{|z_{ij}|} \times \theta\left(\frac{z - z_i}{z_{ij}}\right)\theta\left(\frac{z_{ij}}{z_j - z}\right)\right\rangle, \qquad (3)$$

where $\rho(z)$ is the density profile along the *z*-direction, k_B Boltzmann's constant, *T* the temperature, $A = L_x \times L_y$ is the area of one interface, x_{ij}, y_{ij}, and z_{ij} are the *x*-, *y*-, and *z*-components of the distance r_{ij} between atoms *i* and *j*, respectively, $\langle\cdots\rangle$ denotes the canonical ensemble average, $U_{int.}$ is the potential energy, and $\theta(z)$ is the Heaviside step function.

The components of the pressure tensor are computed by dividing the simulation box into N_{slabs} slabs, parallel to *x*-*y* interface, and the contribution of each interaction between atoms *i* and *j* to the interfacial tension (including bond constraints from the SHAKE algorithm) is distributed in the slabs involved, i.e., slabs in which the particles *i* and *j* reside and slabs in between (Nijmeijer et al., 1988).

Structure analysis

Peptide shape and orientation

To study the dynamics of surfactin molecules as a function of interfacial concentration, we have computed: the trajectory of the center of mass of the surfactin's head (thus, all the atoms except those involved in the fatty-acid chain), its lateral diffusion, and the averaged distance between the centers of mass to estimate the molecular area.

Fig. 1 shows the tridimensional structure of the surfactin molecule in which the peptide part takes the form of a ''horse-saddle.'' This structure can be modeled by a tetrahedron, build from four atoms from the cyclopeptide backbone (see legend to Fig. 1). To characterize the shape and orientation of this horse-saddle we have introduced the vectors $\vec{S}_{top}$, $\vec{S}_{base}$, and $\vec{S}_{height}$ and the dihedral angle $\alpha_{dih.}$. The magnitude of the vectors $\vec{S}_{top}$, and $\vec{S}_{base}$ characterizes the degree of opening of the hydrophilic and hydrophobic side of the horse-saddle, respectively. The rotation of the surfactin molecule is described by the orientation of the $\vec{S}_{height}$ vector. In the case of a tetrahedral structure, $\vec{S}_{height}$ vector is orthogonal to the two orthogonal vectors $\vec{S}_{top}$ and $\vec{S}_{base}$. Thus, the orientation of the $\vec{S}_{height}$ vector can be defined as a sum of

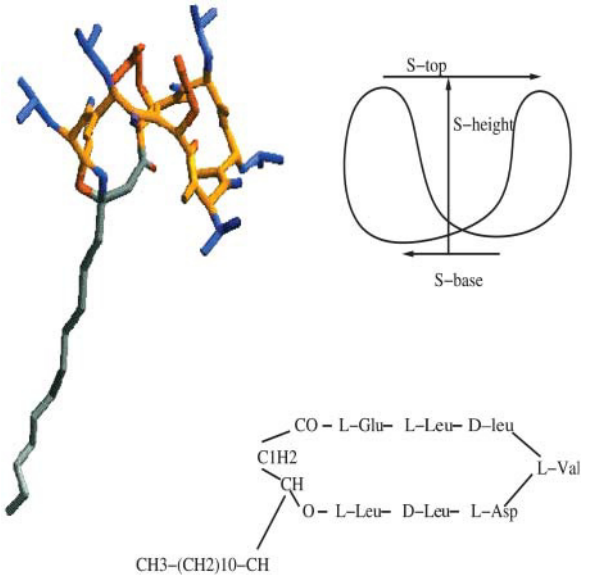

FIGURE 1 Modeling and parameterization of the ''horse-saddle'' conformation. From four atoms defining a tetrahedric structure, **C**O(5), **N**H(2), **C**H(4), and $\mathbf{C}_1$H, are defined three vectors: $\vec{S}_{top}$: **C**O(5) → **N**H(2), $\vec{S}_{base}$: $\mathbf{C}_1$H → α**C**H(4), and $\vec{S}_{height}$: [**C**O(5) − **N**H(2)] → [$\mathbf{C}_1$H − α**C**H(4)]. The dihedral angle $\alpha_{dih.}$ is defined by the angle between two vectors normal to two sides of the tetrahedron, each containing three atoms (**N**H(2)-α**C**H(4)-**C**O(5)) and (α**C**H(4)-**C**O(5)-$\mathbf{C}_1$H), respectively.

contributions from the vectors $\vec{S}_{top}$ and $\vec{S}_{base}$. A negative value of $\vec{S}_{height}$ orientation toward the interface corresponds to a tumbling over of the peptidic part of the surfactin molecule. The dihedral angle $\alpha_{dih.}$ characterizes the horse-saddle shape which can be modeled by a tetrahedron. It corresponds to the angle between the two vectors normal to two faces of the tetrahedron (see legend of Fig. 6). A symmetrical horse-saddle shape yields an angle $\alpha_{dih.}$ of ~74–75°. A change in the sign of $\alpha_{dih.}$ corresponds to an inversion of the horse-saddle conformation, and a value close to 0 corresponds to a flat structure.

Secondary structure

In our simulations, we observe that the surfactin structure may fluctuate depending on the molecular orientation and the interfacial concentration. We have computed Ramachandran angles and hydrogen bonds (intramolecular, and intermolecular between surfactins, and with the solvent) to describe the secondary structure of the surfactant molecule and its flexibility, and to detect secondary structures as γ- and β-turns.

Hydrogen bonds are described from parameters specific to proteins (Thornton et al., 1993; MacDonald and Thornton, 1994). These criteria are a maximum distance of 2.5 Å between H (hydrogen atom) and A (hydrogen acceptor) and a minimum angle of 90° for A···Ĥ-D (hydrogen donor) when A, H, and D coordinates are available. Such criteria allow a complete screening of the most common hydrogen bonds found in proteins but may underestimate bonds involved in particular secondary motifs such as γ- and β-turns, and main-chain lateral-chain interactions. Moreover, we have extended the class of hydrogen bond acceptors to the main-chain nitrogen atom as described in a previous theoretical study (Llamas-Saiz et al., 1992).

Rotational and lateral diffusion

The lateral diffusion coefficient (D_T) has been obtained from the mean square displacement of the center of mass of the peptidic moiety. At long times the diffusion coefficient is:

$$D_T = \lim_{t\to\infty} \frac{1}{2d \times t} \langle |\mathbf{r}(t) - \mathbf{r}(0)|^2 \rangle, \quad (4)$$

where $\mathbf{r}(t)$ is the position of the peptide center of mass at time t, and d the spatial dimension of the displacement. In our case, we have studied surfactant molecules remaining in the planar oil/water interface, hence, we have computed the two-dimensional (translational) diffusion coefficient.

The calculation of the rotational diffusion coefficient is based on the Debye theory (Debye, 1945) which assumes a very diluted solution of rigid dipoles with Brownian motion rotating in a nonpolar media. Application of the theory has been extended to more complex systems and good results have been obtained for protein/water systems (Smith and van Gusteren, 1994). The rotational diffusion coefficient (D_R) can be obtained from the relation:

$$\langle P_l[\cos\theta(t)] \rangle = e^{-l(l+1)D_r t} = e^{-t/\tau_l}, \quad (5)$$

where $\theta(t)$ is the angle between two $\vec{S}_{height}$ vector orientations spaced in time by t, P_l is the l^{th} rank Legendre polynomial, and τ_l the rotational relaxation time associated with each of the Legendre polynomial correlation functions. For molecules undergoing Debye diffusional rotation, a plot of $1/\tau_l$ against $l(l + 1)$ should be linear with a slope equal to D_R.

RESULTS AND DISCUSSION

In this section, we first analyze the behavior of surfactin molecules at the interface through the study of density profiles and center of mass motions of the cyclopeptide moiety. Next the secondary structure of the peptidic part are analyzed, and finally, we relate our results to interfacial properties.

Behavior at the interface

Density profiles

From atomic density profiles plotted in Fig. 2 *A* we observe that surfactin molecules reside at the hexane/water interface. A coordinate analysis of the terminal methyl group of the aliphatic chain (not shown) shows an anchoring of the

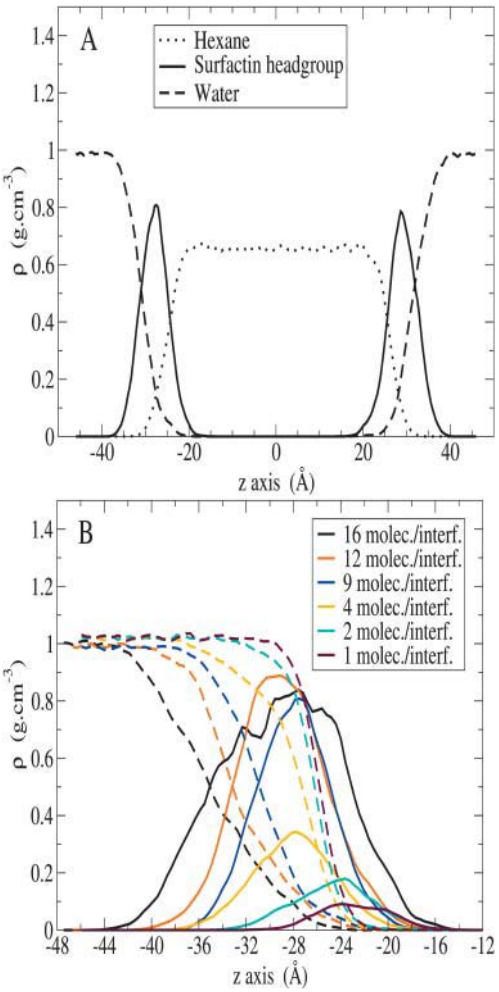

FIGURE 2 Density profiles at 303 *K*. (*A*) Hexane (*straight line*), water (*dashed line*), and surfactin headgroup (*dotted line*) at a concentration of nine surfactins per interface. (*B*) Surfactin (*dotted line*) and water (*dashed line*) profiles at one interface for the different interfacial concentrations: 16, 12, 9, 4, 2, and 1 surfactins per interface.

surfactin molecule in the oil phase. For the three lower concentrations, the surfactin density is increasing with the interfacial concentration, while for the three higher concentrations, the increase of the concentration yields a widening of the surfactin density peak combined with a smoother water interface, as shown in Fig. 2 *B*. This broadening suggests that the organization of the surfactant layer has changed with surfactin molecules slightly popping out of the surfactant monolayer.

Center of mass motions

The projection of the center of mass displacement onto the plane of the interfaces is shown in Fig. 3 for low concentrations and in Fig. 4 at high concentrations. From those snapshots, we observe that molecules exhibit a gaslike behavior with uncorrelated motions below a concentration of four molecules per interface, a solidlike behavior with collective motions above a concentration of 12 molecules per interface, and a liquidlike behavior for intermediary concentrations. This behavior is confirmed by the study of the distance between two surfactin molecules placed at the same interface (not shown). This distance is rather constant at high concentrations but fluctuates at lower concentrations. At the concentration of four surfactins per interface, Fig. 3 *C*, where four molecules are located at each interface in the simulation box, few molecules are clustered. Within a cluster, molecules can be surrounded by one or two neighboring molecules. Molecules are spaced by a minimal distance which decreases from ~15 Å at a concentration of four molecules per interface to less than 10 Å at the highest concentration. These intermolecular distance fluctuations suggest a conformational flexibility of the peptidic moiety. Intermolecular distances yield an estimation for areas which fluctuate from 177 Å^2 at a concentration of four molecules per interface, where the interface is not completely covered by surfactant but few molecules are already in contact, to 78 Å^2 at the highest concentration where we observe the onset of a solid phase. Our results are similar to A_0 and A_t molecular areas obtained from π-*A* isotherms (Ishigami et al., 1995) at pH 4.2, where the surfactin molecule is fully protonated, equal to 184 and 89 Å^2, respectively.

As we will demonstrate next, the properties of the surfactin molecules strongly depend on the aggregation state and their orientation.

Radial distribution functions

Fig. 5 *A* shows the radial distribution functions of the centers of mass of the peptidic part of surfactin molecules. The first peak is observed at ~12, 11.5, 9.5, and 9–12 Å at a concentration of 4, 9, 12, and 16 molecules per interface, respectively, corroborating a compression of surfactin molecules as the interfacial concentration increases. Radial distribution functions have been computed from the projection of the center of mass coordinates onto the interface. As a consequence, molecules popping out of the interface yield minor peaks placed at distances shorter than 8 Å and contribute to a broadening of the peaks. Moreover, the radial distribution functions plotted in Fig. 5 are an average from the contributions of the two interfaces. As a consequence, at the highest concentration, the contribution from the most ordered interface is counterbalanced by the contribution from the other interface, which is less ordered, yielding a radial distribution function not representative to an ideal bidimensional solid.

Molecular shape and orientation

Fig. 6 displays the fluctuations of the $\alpha_{dih.}$ angle related to the tetrahedral shape model of the molecule. At all surface concentrations, the angle distributions exhibit a main peak,

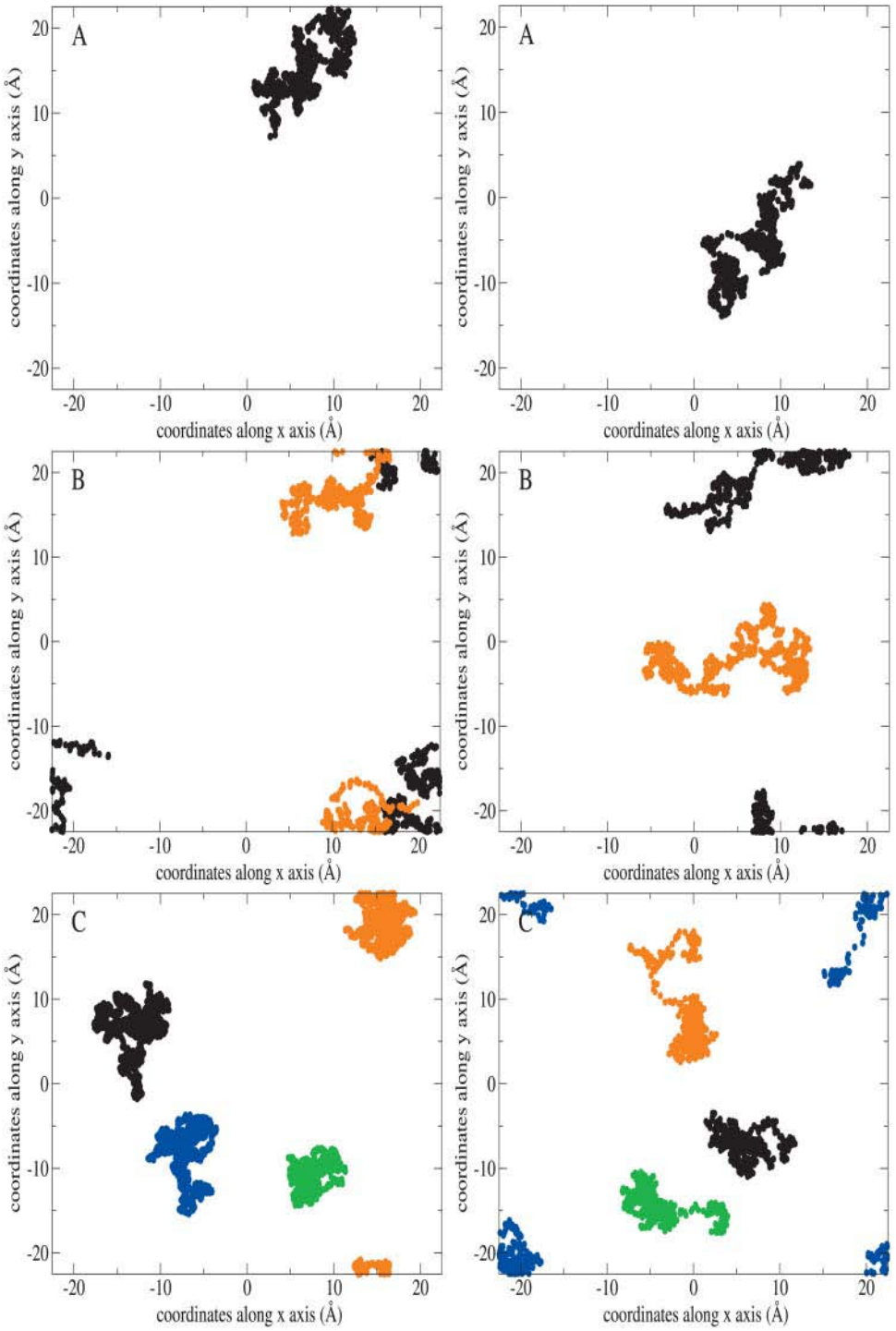

FIGURE 3 Projection of the center of mass of each peptidic moiety at various concentrations. Each molecule center of mass at an interface differs by a color. Each box represents the *x-y* plane and periodic boundary conditions have been applied on coordinates, with (*A*) one, (*B*) two, and (*C*) four surfactins per interface for each interface (*left* and *right*).

sharp and centered on 80–85° at high concentrations (Fig. 6 *A*), and broader with a few other contributions which depend on the orientation of molecules and their environment at low concentrations (Fig. 6 *B*). At low concentrations, molecules can be described as clustered or free (the latter may tumble over). On the one hand, free molecules not tumbled over have a rather flexible tetrahedral shape; on the other hand, clustered or tumbled-over free molecules exhibit a stable $\alpha_{\text{dih.}}$ angle equal to 50–55° and 80–85°, respectively, as shown on Fig. 6 *C*. However, such a $\alpha_{\text{dih.}}$ angle range demonstrates that surfactin molecules at the water/hexane interface adopt a tetrahedral shape, which is similar to the compact ''horse-saddle'' conformation observed under particular conditions (Bonmatin et al., 1994) where surfactin was in a DMSO solution. The amplitude of the observed dihedral angle distributions ascertains the flexibility of the

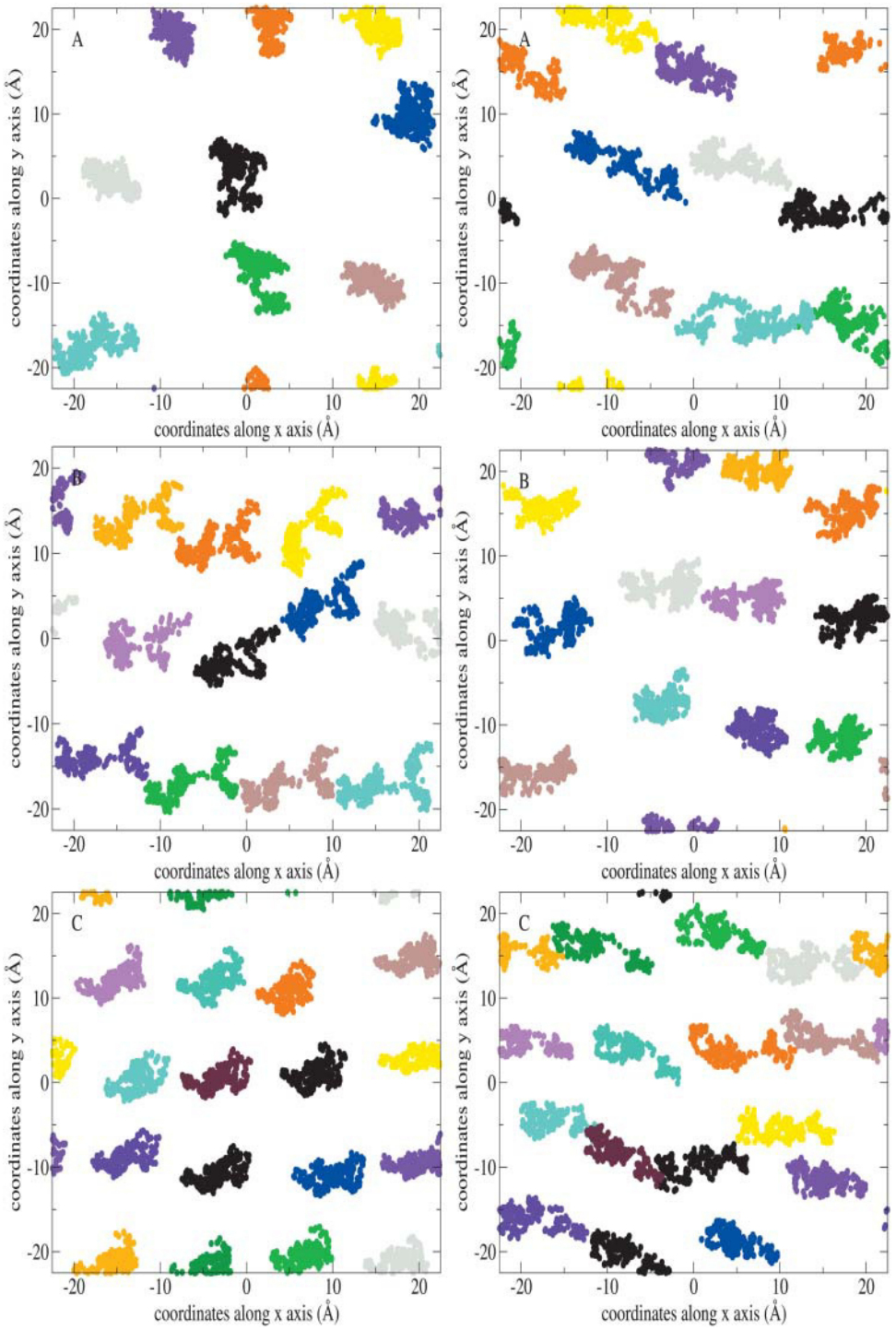

FIGURE 4 Projection of the center of mass of each peptidic moiety at various concentrations. (*A*) 9, (*B*) 12, and (*C*) 16 surfactins per interface for each interface (*left* and *right*).

secondary structure which never remains flat or adopts a reversed saddle shape.

To characterize the orientation of the molecule, i.e., the saddle up or down, we have computed the angle between $\vec{S}_{\text{height}}$ and the *x-y* plane, parallel to the two hexane/water interfaces. At high concentrations, Fig. 7 *A* shows angular distributions in a range of 15–90° with minor contributions <15°. At 16 molecules per interface, the distribution is rather large and centered ~45°, whereas at a concentration of nine molecules per interface the distribution is made of a main peak with a mean angle value of 70°. When the interfacial concentration is increased, the surfactin solidlike molecules popping out of the planar interface may adopt a tilted orientation but have less freedom to tumble. Fig. 7, *B* and *C* illustrate that for concentrations below four molecules per interface, molecules may tumble over. At low concentra-

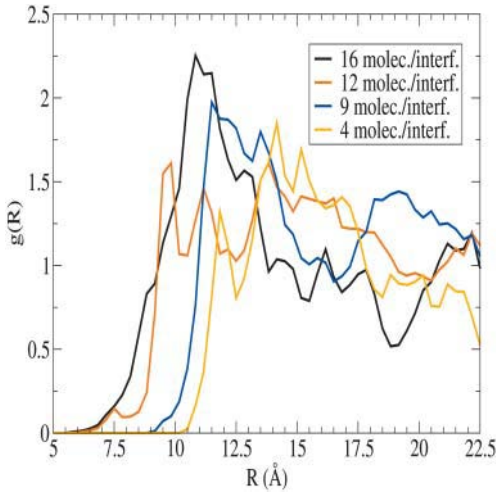

FIGURE 5 Radial distribution function of the center of mass of the peptidic moiety at 4, 9, 12, and 16 surfactins per interface.

tions, the proportion of tumbled-over molecules (corresponding to a negative angle value) increases inversely with the concentration. During our recorded simulations, we have observed one tumbling-over motion within a few tens of picoseconds. That means that the other observed tumbled molecules have tilted during the equilibration time. Moreover, at the concentration of two molecules per interface, we have observed at an interface, two molecules clustered with opposite orientation, forming a kind of ''dimer.''

The tumbling of molecules is a surprising result as compared to previous models proposed from the molecular structure and experiments suggesting that hydrophilic amino acids were oriented toward the hydrophilic part and the hydrophobic part was pointing to the hydrophobic medium or laying at the interface (Ishigami et al., 1995; Bonmatin et al., 1994; Peypoux et al., 1999). First, our results cannot be compared with a previous computed simulation study of surfactin conformation (Gallet et al., 1999) where the interface was defined by the position of the hydrophilic and hydrophobic baricenters in a medium of intermediate dielectric constant. Furthermore, at low interfacial concentrations, lateral chains from the two hydrophilic residues of tumbled-over molecules point into the core of the peptide-avoiding interactions with the hydrophobic oil interface. This phenomenon has been ascertained by the orientation of the lateral chains (not shown) and the existence of hydrogen bonds as shown subsequently. Moreover, the low flexibility of tumbled molecules supports this model of a compact structure.

The global orientation of the molecule given by $\vec{S}_{\text{height}}$ orientation can be explained in terms of the orientation of the two vectors $\vec{S}_{\text{top}}$ and $\vec{S}_{\text{base}}$ placed at the base and the top of the tetrahedral model. At low concentrations, Fig. 8 *B* (*left*) shows a broad distribution centered on a mean value of 15° for the $\vec{S}_{\text{base}}$ angle with a contribution in the range of 30–60° for tumbled-over molecules, whereas at higher concentra-

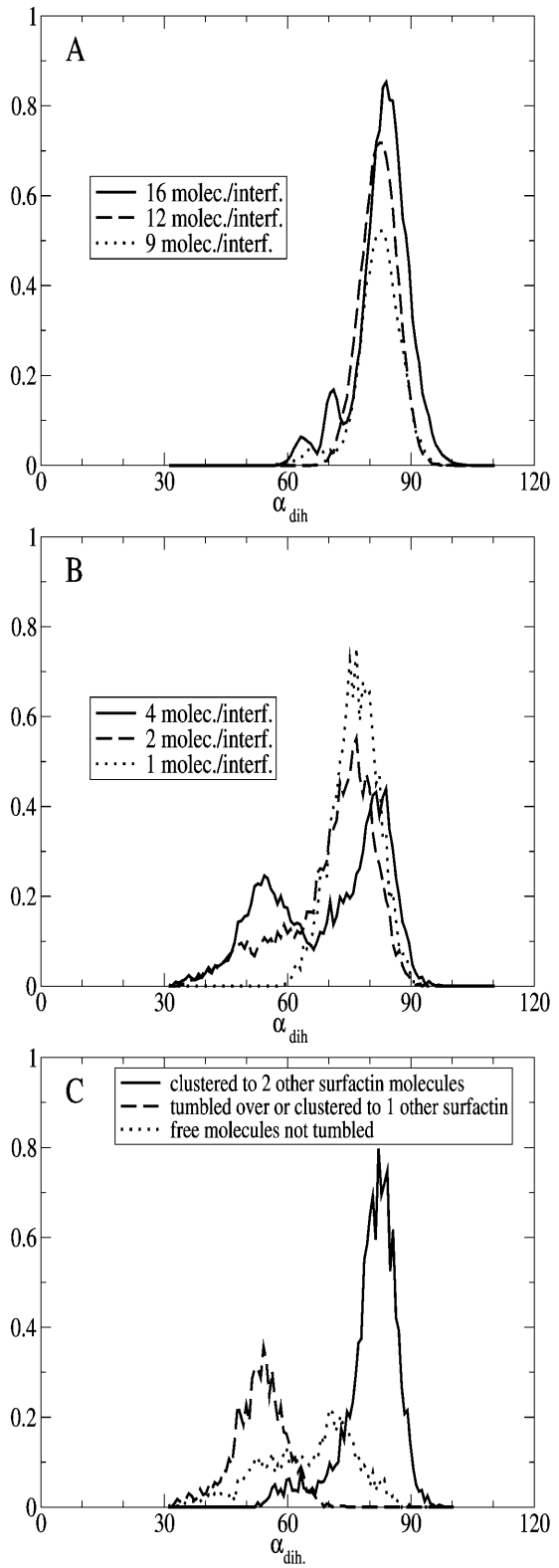

FIGURE 6 Normalized distributions of the $\alpha_{\text{dih.}}$ angle at various interfacial concentrations. (*A*) 9, 12, and 16 surfactins per interface; (*B*) 4, 2, and 1 surfactins per interface; and (*C*) at a concentration of four surfactins per interface plotted with the contributions of molecules clustered with two neighbors (*straight line*), clustered with one neighbor, free and tumbled-over (*dashed line*), and free molecules (*dotted line*).

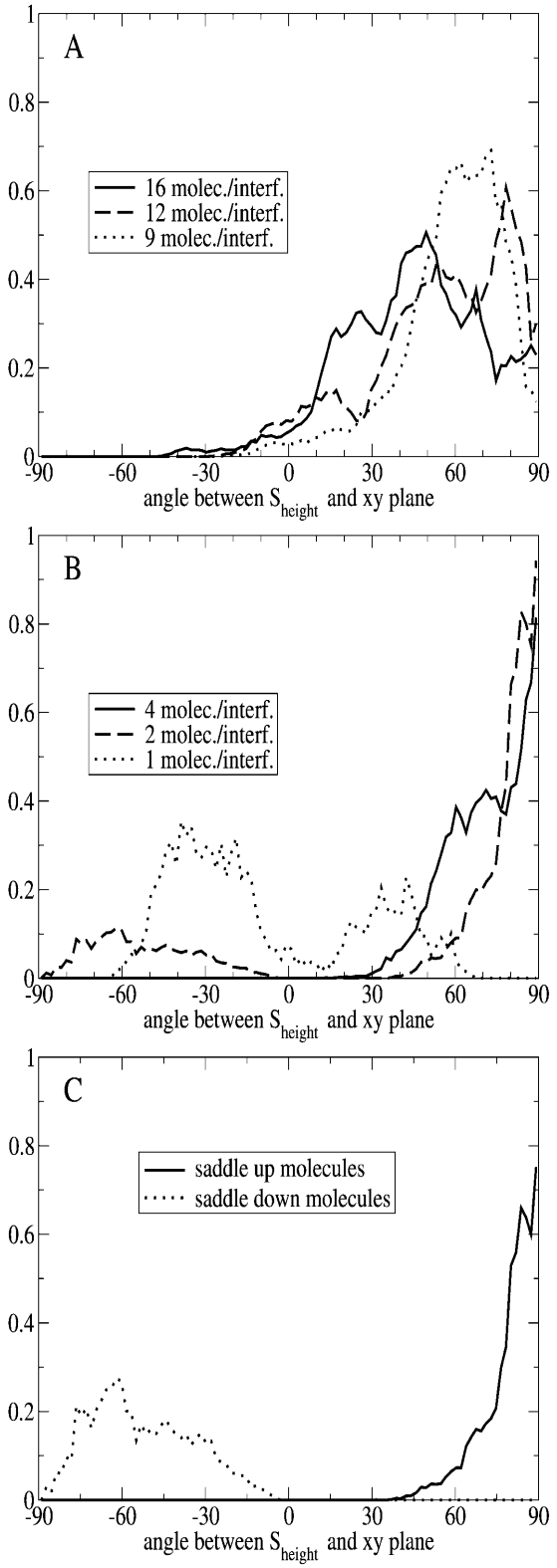

FIGURE 7 Normalized distributions of the $\vec{S}_{\text{height}}$ angle at various interfacial concentrations. (*A*) 9, 12, and 16 surfactins per interface; (*B*) 4, 2, and 1 surfactins per interface; and (*C*) at a concentration of two surfactins per interface plotted with contributions from tumbled-over molecules (*dotted line*) or not (*straight line*).

tions (Fig. 8 *A*, *left*) the distribution is broader. At low concentration, the hydrophobic interface is a plane, whereas at higher concentrations molecules are packed and thus create a hydrophobic environment for those neighboring. In Fig. 8 (*right*) we show fluctuations of the $\vec{S}_{\text{top}}$ vector orientation. The angle distribution is drifting toward low angle values as the interfacial concentration is decreasing. At high concentrations, the angle is ~50°. This behavior confirms the influence of the aggregation on the orientation of the molecules.

Internal dimensions of the tetrahedral structure

The magnitudes of the three vectors $\vec{S}_{\text{top}}$, $\vec{S}_{\text{base}}$, and $\vec{S}_{\text{height}}$ give a complementary insight into the geometry of the surfactin molecule. The $\vec{S}_{\text{height}}$ vector magnitude varies from 2.9 to 4.9 Å as the secondary structure fluctuates (details not shown). Fig. 9 shows the $\vec{S}_{\text{base}}$ and $\vec{S}_{\text{top}}$ magnitude distributions versus the surfactin concentration. Above four molecules per interface, the magnitude is ~5.6 Å, and 4.1 Å for the $\vec{S}_{\text{base}}$ and $\vec{S}_{\text{top}}$ vectors, respectively. At low concentrations, the $\vec{S}_{\text{base}}$ magnitude distribution is broad with a mean value of 6.5 Å, and the $\vec{S}_{\text{top}}$ magnitude distribution shows a broad peak ~6 Å and a sharper one ~4.1 Å, almost separated. At the lowest concentrations, where one molecule is upside down and the other one is tumbling, only the sharp peak is present in Fig. 9 *B* (*right*). In conclusion, concerning the free molecules, the hydrophilic peptidic part is compact when the molecule is tumbled over and its opposite side has an opened conformation. In this case, the $\vec{S}_{\text{base}}$ magnitude distribution reported on Fig. 9 *B* (*left*) has only one broad component due to the lactone part. This has a large ability to fluctuate compared to an amino acid residue. At the intermediate concentration of four molecules per interface, both distributions have a second component. The separation between the two components in Fig. 9 *B* (*right*) demonstrates the existence of two distinguishable conformational states of the hydrophilic side, ''opened'' or ''closed.'' Clustered molecules surrounded by two neighbors are in a ''closed'' conformation while the others, in contact with <1 neighbor, are in an ''opened'' state. Two phenomena can explain this observation. The transition from one state to the other obeys internal constraints and needs a significant activation energy, or the first transition state during the molecular opening adopts a geometry dependent on the first inserted molecule (as a water molecule in our case). However, the ''closed'' state of the hydrophilic side is observed in two cases, at a concentration of four surfactins per interface when molecules are clustered, and at lower concentrations when molecules are upside down. These occurrences suggest strongly that the ''closed'' conformation of the hydrophilic side is stabilized by internal hydrogen bonds favored when interactions of the hydrophilic part with the aqueous phase

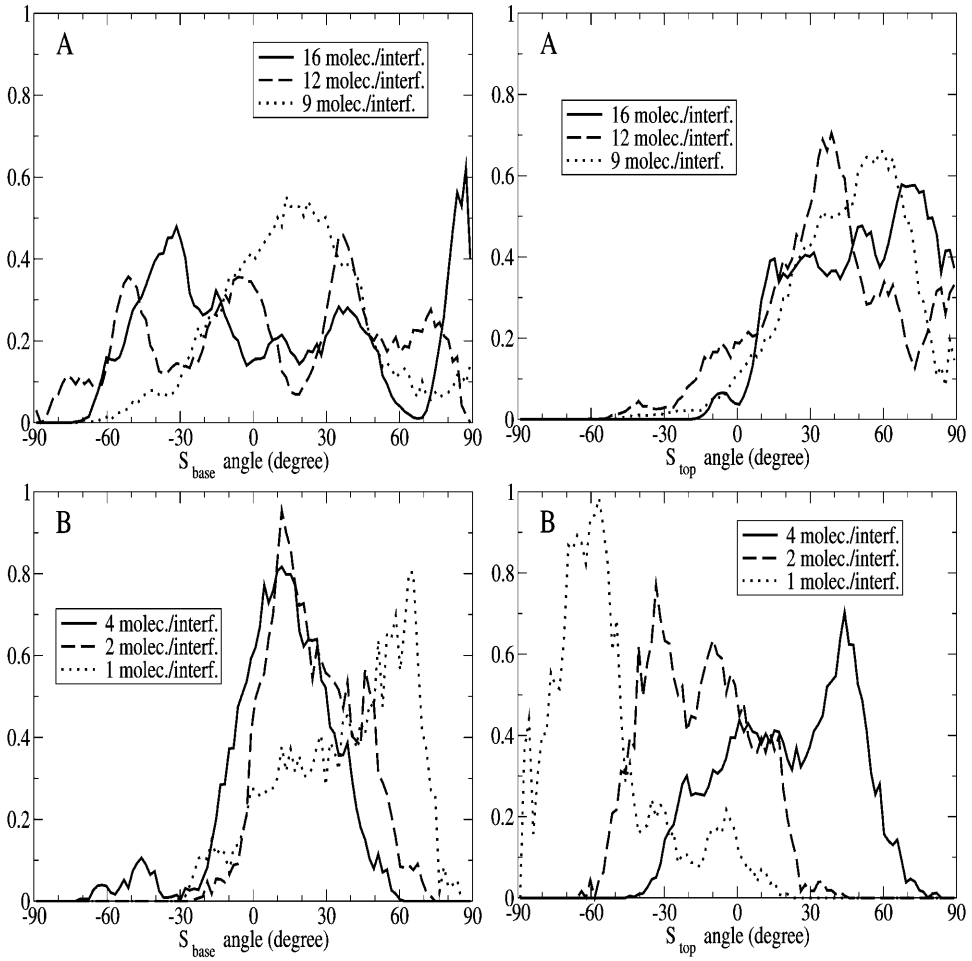

FIGURE 8 Normalized distributions of the angle between $\vec{S}_{base}$ (*left*), $\vec{S}_{top}$ (*right*), and the *x*-*y* plane parallel to the interface. (*A*) 9, 12, and 16 surfactins per interface; (*B*) 4, 2, and 1 surfactins per interface.

are concealed or hindered by the environment by tumbling or packing of the peptidic part, respectively.

Ramachandran angles

To complete the structure analysis and estimate the flexibility of surfactin molecules, we have recorded fluctuations of Ramachandran angles. At concentrations <12 molecules per interface, upside-down molecules have stable Ramachandran angles for all the residues except the terminal ones which are sensitive to the motions of the aliphatic tail and the lactone group. Moreover, those molecules exhibit the Ramachandran angles characteristic of a type II′ β-turn *Asp*5 → *Leu*2. At a concentration of two and four molecules per interface, the free molecules and those clustered with only one neighbor are rather flexible and do not contain a particular structural motif. At a concentration of nine surfactins per interface, about one-third of the molecules are unstable when we consider the Ramachandran angles. They correspond to the molecules which are not yet part of an homogeneous surfactant monolayer.

At a concentration of 12 surfactins per interface, four molecules in total have few unstable angles corresponding to a *D-Leu*3-*Val*4 peptide-plane flip with a (ϕ_4; ψ_3) transition from (−90; −100) to (70; 100), the former state corresponding to the type II′ β-turn and the latter one being metastable. This kind of peptide-plane flip is in agreement with previous work on peptide-plane motions (Hayward, 2001), although it does not correspond to a transition between two stable conformations. With the exception of one molecule containing a *cis D-Leu*3-*Val*4 conformation, all the other molecules have a type II′ β-turn conformation.

At the highest concentration, one-third of the molecules have unstable Ramachandran angles. Of the remaining two-thirds, three molecules exhibit a peptide-plane flip as described above and four molecules adopt a nonconventional turn with (72 ± 12; –100.5 ± 5.7) and (–137 ± 7; 40.25 ± 9.1) as (ϕ_3; ψ_3) and (ϕ_4; ψ_4), respectively, which does not fall into allowed regions of the Ramachandran plot specific to each residue (Hovmöller et al., 2002). The remaining molecules contain a type II′ β-turn. This unexpected conformation found at this concentration may result from the large lateral pressure applied on the surfactin molecules, inducing a conformational transition.

Angular fluctuations may explain the ''chimeric'' character of the molecule (Vass et al., 2001) observed experimentally.

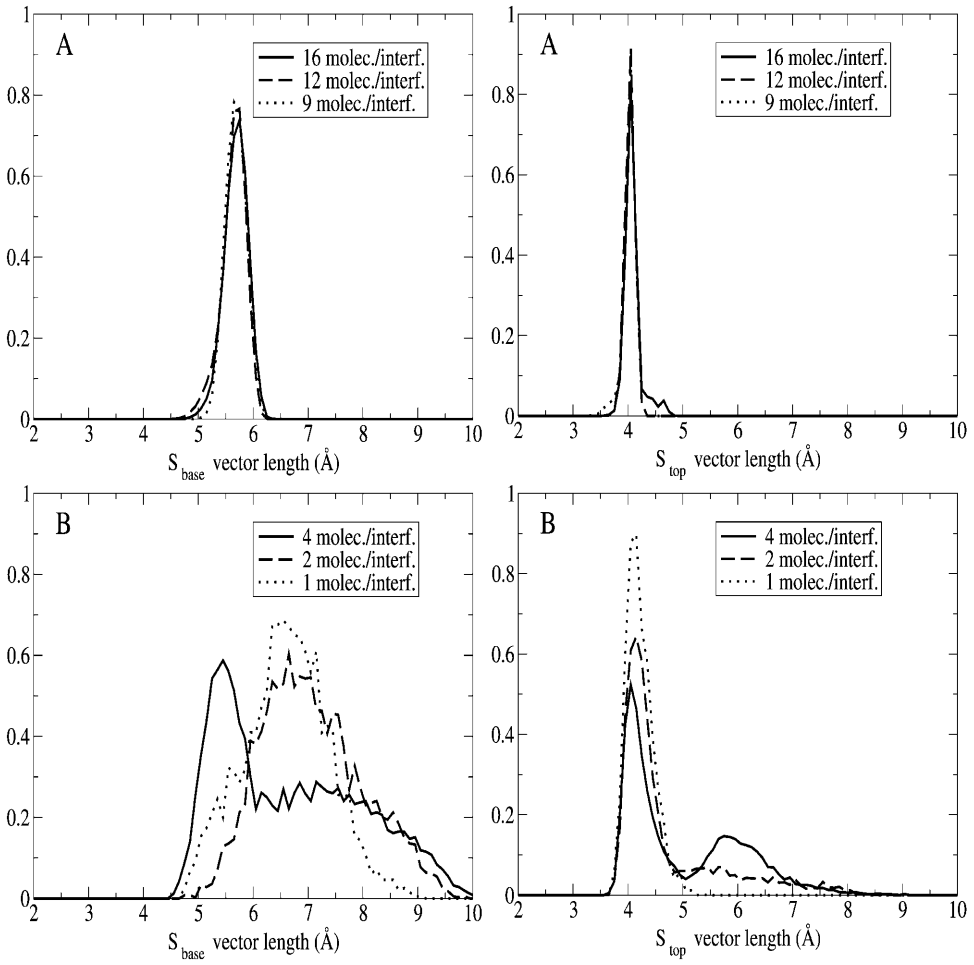

FIGURE 9 Normalized distributions of the $\vec{S}_{base}$ (*right*) and $\vec{S}_{top}$ (*left*) vector magnitude at various concentrations. (*A*) 9, 12, and 16 surfactins per interface; (*B*) 4, 2, and 1 surfactins per interface.

Motions of the peptidic backbone, as the coexistence of different conformers under identical physical conditions, induce a large distribution of the amide and the carboxylic groups orientation, yielding different absorption spectroscopic characteristics. But despite this angular variability, all the molecules at concentrations greater than four molecules per interface, have a similar hydrogen bond network we now show.

Intramolecular hydrogen bonds

In Fig. 10, *A* and *B*, we illustrate the contributions of the most frequent intramolecular hydrogen bonds observed, excluding hydrogen bonds within carboxylic functions, at concentrations of four and two surfactins per interface, respectively. Three hydrogen bonds have an occurrence probability longer than half of the simulated time. They are two ''weak'' bifurcated hydrogen bonds, NH(1)-CO(5) and NH(2)-CO(5), and the hydrogen bond characteristic of the conformer S1, NH(5)-CO(2). Those bonds mainly occur within packed or upside-down molecules. It is worth noticing that those bonds, as defined by the method outlined above, are also detected from the coordinate set of conformer S1.

When focusing on less frequent hydrogen bonds, we notice that the *Glu*1 carboxylic group is more often involved in intramolecular hydrogen bonds than the *Asp*5 carboxylic group. This can be explained by the length of the *Glu*1 lateral chain being larger than its analog in the *Asp*5 residue allowing a greater flexibility. The oxygen atoms from *Glu*1 interact preferentially with NH(7) and NH(1) while the rare bonds involving *Asp*5 concern NH(5). Most of the molecules which are upside down have a hydrogen bond between *Glu*1 and CO(7) too. Such interactions confirm the insertion of the carboxylic group in the peptide core when its residue is shielded from the hydrophilic medium. Finally, most of the molecules which are not stabilized by the three most abundant hydrogen bonds present various weak hydrogen bonds such as NH(5)-NH(4), NH(3)-NH(2), NH(2)-NH(1), and NH(3)-CO(1) with various occurrence probabilities (from 10 to 30%).

At concentrations of 9, 12, and 16 surfactins per interface, the two hydrogen bonds NH(2)-CO(5), and NH(5)-CO(2) have an occurrence probability almost equal to the recorded time as NH(7)-COOH(1). Thus, albeit few molecules have conformational transitions as illustrated by their Ramachandran angle analysis, the type II′ β-turn hydrogen bonds are

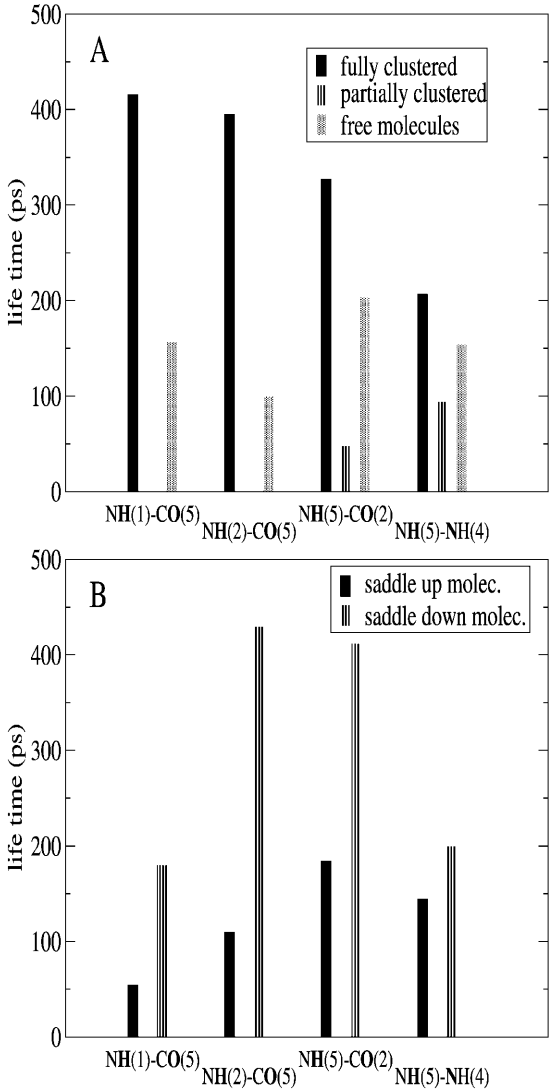

FIGURE 10 Most frequent hydrogen bonds. (*A*) At high concentration for fully clustered molecules surrounded by more than one neighbor molecule (*black sticks*), partially clustered molecules in contact with only one neighbor (*dashed sticks*), and free molecules (*gray sticks*); and (*B*) at mean concentration for saddle-up (*straight sticks*) and saddle-down (*gray sticks*) molecules.

preserved. Moreover, we observe few other hydrogen bonds rather stable as NH(5)-NH(4), NH(1)-CO(5), and COOH(1)-CO(7).

Whatever the concentrations, we have never noticed hydrogen bonds between the two different carboxylic groups of a single molecule. Moreover, in any cases studied we have detected one of the three hydrogen bonds characteristic of the S2 conformer, NH(7)-CO(5), NH(4)-CO(2), and NH(6)-C^1O. This suggest that no transition is allowed from S1 conformer to S2 conformation under the physical conditions used for our simulations. On the other hand, we have performed simulations starting from the S2 conformer. The characteristic structural parameters of this conformation that contains two γ-turns have not been conserved during the equilibration period. This confirms the S1 conformer as the most stable conformation at a hydrophilic/hydrophobic interface at a wide range of interfacial concentrations.

Interactions between a surfactin and its environment

The peptide is not big enough to have buried hydrogen acceptors or donors and only a few nitrogen and oxygen atoms were part of intramolecular hydrogen bonds. This suggests clearly that most of the remaining oxygen and nitrogen atoms interact with the solvent or other surfactins as hydrogen bond donor or acceptor.

In fact, very few hydrogen bonds between surfactin molecules have been detected. During the simulation, bonds involving the *Asp*5 carboxylic group, and CO(1) and CO(2) groups, between two aggregated molecules at an interface, and the *Glu*1 carboxylic group, and CO(6) and O(lactone) groups, between two other associated molecules at the other interface, have been identified at the highest surfactin concentration. However, these binding associations have rather different occurrence probabilities, at 3.5% and 32.2%, respectively.

Hydrogen bonds between surfactin and water molecules are numerous. We have investigated hydrogen bonds involving a water molecule and two residues and classified them as type I, II, or III depending on the geometry of the interaction between the water molecule (Hw-Ow-Hw) and the hydrogen bond donor (D) and acceptor (A), D-(Ow)-D, D-(Ow-Hw)-A, A-(Hw-Ow-Hw)-A, respectively. We assume that the donors and acceptors which are not involved in one of the previously described intra- and intermolecular hydrogen bonds interact with a single water molecule as D-Ow, A-Hw.

Most of the intermolecular hydrogen bonds have a probability <5%. But when we focus on the most stable bonds, we notice that hydrogen bonds from the type I are encountered between two consecutive amino acids NH(n)-NH(n + 1) in the less compact surfactin molecules. Their occurrence probabilities are in the range of 30–60%. Hydrogen bonds from type II are the most abundant except for molecules that are upside down. In this case, one of the most stable hydrogen bonds is linking the *Glu*1 carboxylic group and CO(7). This bond can have a probability up to 100%. The less compact molecules are stabilized by a large number of hydrogen bonds of this type. The most specific bonds are between NH(1) or NH(2) and CO(5). Their occurrence probabilities are in a range of 10–100%. Their presence is closely related to the increase of the ''top'' vector magnitude. As a consequence, compact molecules rarely have hydrogen bonds from type II and none of them seems to be stable within this molecular geometry. The last type of hydrogen bonds, type III, is rather abundant. In packed molecules, bonds between CO(4)-CO(6) and CO(3)-C_1O

have a probability of 75 and 60%, respectively, while this value decreases dramatically for the other molecules, except for molecules which are upside down, where CO(3)-C_1O is more abundant than CO(4)-CO(6).

In conclusion, type I and III hydrogen bonds are mainly linking the peptide with its solvation shell, whereas type II bonds are characteristic of ''opened'' conformations of the hydrophilic moiety and take place between residues involved in the intramolecular hydrogen bonds present in packed molecules.

Interfacial properties

Diffusion coefficients

Rotational diffusion coefficient calculations are based on the motions of the $\vec{S}_{\text{height}}$ vector toward the interfacial plane whereas translational diffusion coefficients are computed from centers of mass displacements. An average of a vector's ensemble motions should give a better description of the rotational behavior. However, this vector is defined from the $\vec{S}_{\text{base}}$ and $\vec{S}_{\text{top}}$ vectors; thus local fluctuations are by definition partially averaged.

In Fig. 11 *A*, $1/\tau_1$ is plotted versus $l(l + 1)$ for all the concentrations. We observe a linear relationship for all concentrations except the lowest one. This result validates the Debye model to describe the rotational motion despite the insertions of the aliphatic tail and the lateral chains from apolar residues in the hydrophobic medium. This likely tail perturbation might be averaged over all the molecules by interactions between amino acid lateral chains and solvents. Concerning the lowest concentration, two phenomena may explain this nonlinear behavior. On the one hand, only two molecules contribute to the value, consequently, the statistical accuracy and validity of the results are quite low. Moreover, one of the two molecules has a fast tumbling-over motion which brings a ''nonconventional'' contribution to the global rotational motion studied. In Fig. 11 *B*, three logarithms of Legendre polynomial correlation functions are displayed. The short-time part of the curves contains some additional structure which could be related to internal motions of the protein and to rattling of the peptidic moiety within the solvent shell. The variation of rotational diffusion coefficient as a function of the interfacial concentration is plotted on Fig. 11 *C*.

Table 1 contains numerical values of both rotational and lateral diffusion coefficients. The rotational diffusion coefficient decreases as the interfacial concentration increases due to the lack of freedom for molecules at high interfacial concentrations. The lateral diffusion coefficient shows a dependence on the concentration from a concentration of 2–4 molecules per interface. At the lower concentration, our results present a poor statistical value. Moreover, the peptidic part of one of the two molecules has tumbled over on itself during the simulation. This rare motion may have affected the averaged value of the lateral diffusion coefficient.

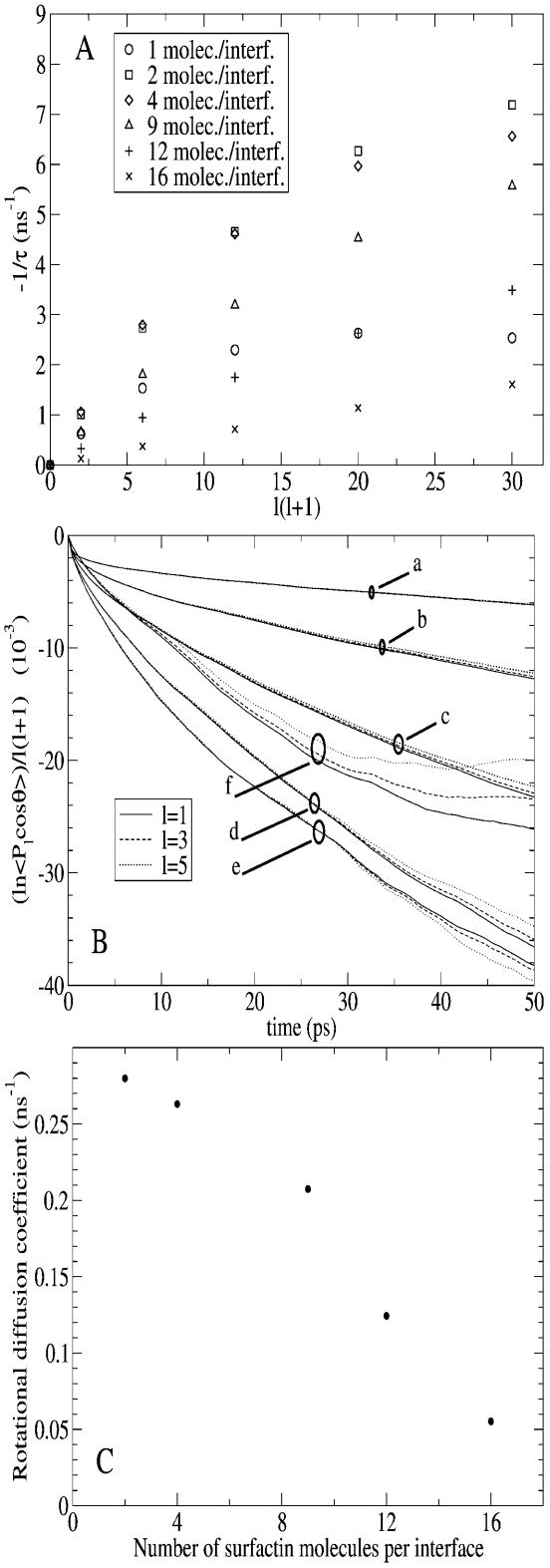

FIGURE 11 (*A*) Inverse of the rotational relaxation time τ_l as a function of $l(l + 1)$ corresponding to the five first Legendre polynomia P_l. (*B*) $\ln\langle P_l[\cos\theta(t)]\rangle$ as a function of time for three Legendre polynomia, P_1, P_3, and P_5, at 16 (*a*), 12 (*b*), 9 (*c*), 4 (*d*), 2 (*e*), and 1 (*f*) surfactins per interface.

TABLE 1 Interfacial tension, rotational and lateral diffusion coefficients as a function of the number of surfactant per interface

Interfacial concentration (mol/interface)	D_T (10^{-12} m^2 × s^{-1})	D_R (ns^{-1})	γ (mN × m^{-1})
0*	–	–	46.0 ± 1.6
1	670 ± 120	–	47.4 ± 1.7
2	950 ± 220	0.280	44.3 ± 1.6
4	320 ± 140	0.263	49.7 ± 1.7
9	260 ± 140	0.207	46.2 ± 1.9
12	230 ± 70	0.124	31 ± 2
16	180 ± 60	0.055	18 ± 2

*Results from previous simulations concerning a hexane-water binary system (unpublished data).

Interfacial tension and tangential pressure profile

From preliminary studies on alkane biphasic systems (Nicolas and Smit, 2002), hexane-water (unpublished data), and nonane/nonanol/water systems (unpublished data), we have shown that this way of performing the interfacial calculation is correct in a large range of temperatures and gives underestimated values (~10–15%) of interfacial tensions compared to experimental results.

Simulated interfacial tensions are reported in Table 1. Up to nine molecules per interface, the interfacial tension is roughly constant. Above this limit, the interfacial tension can decrease dramatically until a minimal value of one-half the interfacial tension of a pure hexane/water system. This decline in the interfacial tension illustrates the surprising interfacial activity of the surfactin molecule and gives an estimation of the ''active'' range of surfactin interfacial concentrations. The efficiency of surfactin in lowering the interfacial tension of a hexane-water system is comparable to its ability to reduce the water-air interfacial tension (Ishigami et al., 1995; Peypoux et al., 1999).

Through the plot of the tangential component of the pressure profile, shown on Fig. 12, we can analyze the effect of surfactin molecules at the interface. At low concentrations, up to four molecules per interface, pressure profiles show a single structured peak. This peak contains contributions from a sharp peak characteristic of the oil/water interface, and a broader one related to the surfactin layer. While the concentration is increasing, direct contacts between oil and water phases are reduced by the surfactant film. At a concentration of nine surfactin molecules per interface, the interface is fully covered by the surfactant layer and the lateral pressure profile contains several peaks. While the concentration is increasing, the profile is broader as the interfacial region is becoming thicker with an increasing number of surfactin molecules slightly popping out of the surfactant layer.

The reduction of the interfacial tension at concentrations higher than nine surfactin molecules per interface (corresponding roughly to the interfacial concentration needed for a total covering of the oil/water interface) results mainly from the contribution of interactions between surfactant molecules which are not fully embedded in the surfactant layer and water or oil phase. They yield a positive contribution to the tangential pressure profile (considering that in the bulk phases, either that of oil or water, the tangential pressure profile is, on average, null).

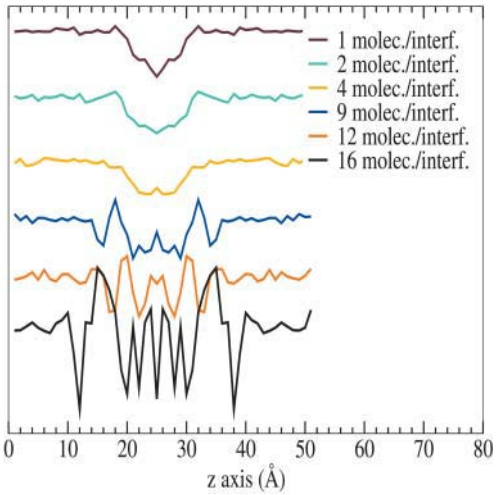

FIGURE 12 Tangential pressure profiles at various concentrations. The oil interface is located at $z \approx 25$ Å, with the oil phase on the right side of the graph, and the aqueous phase on the left side. This plot is an average of the tangential component of the pressure profile of the two interfaces and over a simulation of 0.5 ns.

CONCLUDING REMARKS

These simulations are the first molecular dynamic studies at an atomic level of surfactin in a liquid hydrophilic/hydrophobic environment. They bring an interesting insight into the structural variability of the surfactin molecule depending on interfacial concentration and the molecular environment, and investigate the interfacial properties of this remarkable molecule. Since very few structure-activity correlation studies at an hydrophilic/hydrophobic interface have been carried out experimentally it is difficult to compare our results with existing data. However, the spectroscopic studies done in a homogeneous medium suggest a structural variability depending on the nature of the solvent and concentrations of cations. In our model which reproduces the native environment of the protonated form of surfactin, except its salt concentrations, we demonstrate that the conformation depends also on the environment of the molecule. Structural variabilities have already been observed (Zhong and Johnson, 1992; Li and Deber, 1993) when a peptidic segment was placed in a different medium. In this study, we have demonstrated that placed at the same hydrophilic/hydrophobic interface, the surfactin molecule adopts different conformations depending on its

interfacial concentration. Placed in a crowded environment, molecules are associated such that the interactions between hydrophobic residues and the hydrophilic medium are minimized. Such clusters are mainly stabilized by van der Waals interactions and from time to time by intermolecular hydrogen bonds involving carboxylic lateral chains. Moreover, when hydrophilic residues are shielded from the environment, a complete tumbling over of the peptidic part can occur. This can be related to the ability of a surfactin molecule to go across a hydrophobic medium as a lipid membrane. We hope that our descriptions of the structural variability at this hydrophobic/hydrophilic interface will bring helpful insights for the interpretation of spectroscopic results.

From these results, we can assume other environmental factors such as an organized and charged environment (as a zwitterionic lipid bilayer) will strongly affect the conformation of surfactin molecule and its orientation as suggested by experimental results (Grau et al., 1999).

J.P. Nicolas thanks B. Smit for his helpful comments, J.A.J. Geenevasen and K.J. Hellingwerf for their stimulating discussions, and G. Zwanenburg and C. Lowe for their support.

REFERENCES

Allen, M. P., and D. J. Tildesley. 1989. Computer Simulation of Liquids. Clarendon Press, Oxford, UK.

Arima, K., A. Kakinuma, and G. Tamura. 1968. Surfactin, a crystalline peptide lipid surfactant produced by *Bacillus subtilis*: isolation, characterization and its inhibition of fibrin clot formation. *Biochem. Biophys. Res. Commun.* 31:488–494.

Béven, L., and H. Wróblewski. 1997. Effect of natural amphipathic peptides on variability, membrane potential, cell shape and motility of mollicutes. *Res. Microbiol.* 148:163–175.

Bonmatin, J. M., M. Genest, H. Labbé, and M. Ptak. 1994. Solution three-dimensional structure of surfactin: a cyclic lipopeptide studied by ^{1}H-NMR, distance geometry, and molecular dynamics. *Biopolymers.* 34:975–986.

Debye, P. 1945. Polar Molecules. Dover, New York.

DLPOLY 2.12. 2001. Daresbury Laboratory, Daresbury, Warrington, UK.

Essmann, U., L. Perera, M. L. Berkowitz, T. Darden, H. Lee, and L. G. Pedersen. 1995. A smooth particle mesh Ewald method. *J. Chem. Phys.* 103:8577–8593.

Ferré, G., F. Besson, and R. Buchet. 1997. Conformational studies of the cyclic L,D-lipopeptide surfactin by Fourier transform infrared spectroscopy. *Spectrochim. Acta A Mol. Biomol. Spectrosc.* 53:623–635.

Gallet, X., M. Deleu, H. Razafindralambo, P. Jacques, P. Thonart, M. Paquot, and R. Brasseur. 1999. Computer simulation of surfactin conformation at a hydrophobic/hydrophilic interface. *Langmuir.* 15:2409–2413.

Grau, A., J. C. G. Fernández, F. Peypoux, and A. Ortiz. 1999. A study on the interactions of surfactin with phospholipid vesicles. *Biochim. Biophys. Acta.* 1418:307–319.

Hayward, S. 2001. Peptide-plane flipping in proteins. *Protein Sci.* 10:2219–2227.

Heerklotz, H., and J. Seelig. 2001. Detergent-like action of the antibiotic peptide surfactin on lipid membranes. *Biophys. J.* 81:1547–1554.

Hoover, W. G. 1985. Canonical dynamics: equilibrium phase-space distributions. *Phys. Rev. A.* 31:1695–1697.

Hovmöller, S., T. Zhou, and T. Ohlson. 2002. Conformations of amino acids in proteins. *Acta Crystallogr. D Biol. Crystallogr.* 58:768–776.

Ishigami, Y., M. Osman, H. Nakahara, Y. Sano, R. Ishiguro, and M. Matsumoto. 1995. Significance of β-sheet formation for micellization and surface adsorption of surfactin. *Coll. Surf. B Biointer.* 4:341–348.

Jorgensen, W. L., J. Chandrasekhar, J. D. Madura, R. W. Impey, and M. L. Klein. 1983. Comparison of simple potential functions for simulating liquid water. *J. Chem. Phys.* 79:926–935.

Kameda, Y., S. Ouhira, K. Matsui, S. Kanatomo, T. Hase, and T. Atsusaka. 1974. Antitumor activity of *Bacillus natto*. V. Isolation and characterization of surfactin in the culture medium of *Bacillus natto* KMD 2311. *Chem. Pharm. Bull.* 22:938–944.

Kirkwood, J. G., and F. P. Buff. 1949. The statistical mechanical theory of surface tension. *J. Chem. Phys.* 17:338–343.

Kracht, M., H. Rokos, M. Özel, M. Kowall, G. Pauli, and J. Vater. 1999. Antiviral and hemolytic activities of surfactin isoforms and their methyl ester derivatives. *J. Antibiot.* 52:613–619.

Li, S. C., and C. M. Deber. 1993. Peptide environment specifies conformation: helicity of hydrophobic segments compared in aqueous, organic, and membrane environments. *J. Biol. Chem.* 268:22975–22978.

Llamas-Saiz, A. L., C. Foces-Foces, O. Mo, M. Yañez, and J. Elguero. 1992. Nature of the hydrogen bond: crystallographic versus theoretical description of the O-H$\cdots$N(sp^2) hydrogen bond. *Acta Crystallogr. B.* 48:700–713.

MacDonald, I. K., and J. M. Thornton. 1994. Satisfying hydrogen bonding potential in proteins. *J. Mol. Biol.* 238:777–793.

MacKerell, A. D., Jr., D. Bashford, M. Bellott, R. L. Dunbrack, Jr., J. D. Evanseck, M. J. Field, S. Fischer, J. Gao, H. Guo, S. Ha, D. Joseph-McCarthy, L. Kuchnir, K. Kuczera, F. T. K. Lau, C. Mattos, S. Michnick, T. Ngo, D. T. Nguyen, B. Prodhom, W. E. Reiher III, B. Roux, M. Schlenkrich, J. C. Smith, R. Stote, J. Straub, M. Watanabe, J. Wiórkiewicz-Kuczera, D. Yin, and M. Karplus. 1998. All-atom empirical potential for molecular modeling and dynamics studies of proteins. *J. Phys. Chem. B.* 102:3586–3616.

Maget-Dana, R., and M. Ptak. 1992. Surfactin: interfacial properties and interactions with membrane lipids in mixed monolayers. *Thin Solid Films.* 210:730–732.

Nagai, S., K. Okimura, N. Kaizawa, K. Ohki, and S. Kanatomo. 1996. Study on surfactin, a cyclic depsipeptide. II. Synthesis of surfactin B_2 produced by *Bacillus natto* KMD 2311. *Chem. Pharm. Bull.* 44:5–10.

Nicolas, J. P., and B. Smit. 2002. Molecular dynamics simulations of the surface tension of *n*-hexane, *n*-decane and *n*-hexadecane. *Mol. Phys.* 100:2471–2475.

Nijmeijer, M. J. P., A. F. Bakker, C. Bruin, and J. H. Sikkenk. 1988. A molecular dynamics simulation of the Lennard-Jones liquid-vapor interface. *J. Chem. Phys.* 89:3789–3792.

Osman, M., H. Høiland, H. Holmsen, and Y. Ishigami. 1998. Tuning micelles of a bioactive heptapeptide biosurfactant *via* extrinsically induced conformational transition of surfactin assembly. *J. Pept. Sci.* 4:449–458.

Peypoux, F., J. M. Bonmatin, and J. Wallach. 1999. Recent trends in the biochemistry of surfactin. *Appl. Microbiol. Biotechnol.* 51:553–563.

Razafindralambo, H., Y. Popineau, M. Deleu, C. Hbid, P. Jacques, P. Thonart, and M. Paquot. 1997. Surface-active properties of surfactin/iturin A mixtures produced by *Bacillus subtilis*. *Langmuir.* 13:6026–6031.

Razafindralambo, H., Y. Popineau, M. Deleu, C. Hbid, P. Jacques, P. Thonart, and M. Paquot. 1998. Foaming properties of lipopeptides produced by *Bacillus subtilis*: effect of lipid and peptide structural attributes. *J. Agric. Food Chem.* 46:911–916.

Ryckaert, J.-P., G. Ciccotti, and H. J. C. Berendsen. 1977. Numerical integration of the Cartesian equations of motion of a system with constraints: molecular dynamics of *n*-alkanes. *J. Comput. Phys.* 23:327–341.

Smith, P. E., and W. F. van Gusteren. 1994. Translational and rotational diffusion of proteins. *J. Mol. Biol.* 236:629–636.

Thornton, J. M., M. W. MacArthur, I. K. MacDonald, D. T. Jones, J. B. O. Mitchell, C. L. Nandi, S. L. Price, and M. J. J. M. Zvelebil. 1993. Protein structures and complexes: what they reveal about the interactions that stabilize them. *Phil. Trans. R. Soc. Lond. A.* 345:113–129.

Vass, E., F. Besson, Z. Majer, L. Volpon, and M. Hollósi. 2001. Ca^{2+}-induced changes of surfactin conformation: a FTIR and circular dichroism study. *Biochem. Biophys. Res. Commun.* 282:361–367.

Vollenbroich, D., G. Pauli, M. Özel, and J. Vater. 1997a. Antimycoplasma properties and application in cell culture of surfactin, a lipopeptide antibiotic from *Bacillus subtilis*. *Appl. Environ. Microbiol.* 63:44–49.

Vollenbroich, D., M. Özel, J. Vater, R. M. Kamp, and G. Pauli. 1997b. Mechanism of inactivation of enveloped viruses by biosurfactant surfactin from *Bacillus subtilis*. *Biologicals.* 25:289–297.

Walton, J. P. R. B., D. J. Tildesley, J. S. Rowlinson, and J. R. Henderson. 1983. The pressure tensor at a planar surface of a liquid. *Mol. Phys.* 48:1357–1368.

Zhong, L., and W. C. Johnson, Jr. 1992. Environment affects amino acid preference for secondary structure. *Proc. Natl. Acad. Sci. USA.* 89:4462–4465.